Surface Crack Propagation in SUS304 Stainless Steel Wide Plates under Creep-Fatigue Bending Load

Y. FUKUDA, Y. SATOH
Hitachi Ltd., Hitachi, Japan
K. KASHIMA
CRIEPI, Tokyo, Japan

1. INTRODUCTION

At elevated temperatures where structural materials become non-linear, experimental data sufficient for validating the method of evaluating fatigue crack propagation by non-linear fracture mechanics has not been obtained, also, it is difficult to say that an evaluation method has even been developed. It is thought that J-integral is most suitable as a non -linear fracture mechanics parameter, but it is difficult to experimentally measure J-integrals of structures, even if their configurations are simple at elevated temperatures. Further, the accuracy of this method is not clear. Therefore, it is necessary to study J-integral with elastic-plastic analysis using the 3-dimensional finite element method. This report discribes (1) the experimental and analytical results of 3-dimensional crack propagation in a case where SUS304S.S. wide plates with a part-through crack are subjected to simulated thermal stress bending at 550℃, for FBR components, (2) crack propagation behavior in welded joints, (3) non-destructive measurement of 2-dimenstional crack depth distribution and (4) evaluations of crack growth by J-integral.

This work was carried out as a part of "The verification of evaluation method for structural integrity at high temperature" funded by the Ministry of International Trade and Industry.

2. TEST AND ANALYSIS PROCEDURE

2.1 Test procedure

The test material is hot rolled JIS SUS304 stainless steel plate. Chemical compositions and mechanical properties of the material are shown in Table 1. Specimens are configured to be 50mm thick modeling a sector of the full scale reactor vessel of FBR, 500mm wide and 1600mm long as shown in Fig. 1. The specimens have semi-elliptical slits which are electric-discharge machined on the surface centers. The experiment was conducted on base metal and welded joints in a nominal strain range $\Delta\varepsilon$=0.4% far from the slit. Strain waves were triangular at the strain rate $\dot{\varepsilon}$=0.04%/S and trapezoid with 15 min. hold time in the tensile side.

A 2-dimensional crack configuration was measured by two kinds of non-destructive methods. One was a replication method for the surface length and the other was the Pulse-Potential Drop Method (P-PDM)[1]. The location of input and output terminals in P-PDM are shown in Fig. 2. To obtain data for validating P-PDM after the test, several stripes were marked on the fracture surface by periodical dwell cycling of half the strain range at room temperature.

2.2 Crack propagation analysis procedure

Crack propagation analysis was conducted only in the case of continuous cycling (fatigue) of base metal by 3-dimensional finite element method, J-integral was calculated on 4 different sizes of similar shape cracks in SUS304 stainless steel under the conditions of $\Delta\varepsilon$=0.4% at 550℃.
As the law of material crack propagation, the equation $da/dN=C\cdot\Delta J^n$ was adopteds and constants C and n depending on the material were determined from data obtained from another basic experiment.

An analysis model of a quarter of the specimen is shown in Fig. 3. The model consists of 365 elements of 3-dimensional solids and 1,826 nodes. Elastic -plastic analysis was conducted on the model. J-integrals were calculated using the virtual crack extension method from stress and strain obtained by elastic -plastic analysis. Fig. 7 shows mesh elements containing 4 different size semi -elliptical cracks from which J-integrals were calculated. The crack shapes are described by the following 4 equations.

$$\left.\begin{array}{ll}
(1) & \dfrac{X^2}{40^2}+\dfrac{Y^2}{10^2}=1 \quad \cdots\cdots \text{Case1} \\
(2) & \dfrac{X^2}{60^2}+\dfrac{Y^2}{15^2}=1 \quad \cdots\cdots \text{Case2} \\
(3) & \dfrac{X^2}{80^2}+\dfrac{Y^2}{20^2}=1 \quad \cdots\cdots \text{Case3} \\
(4) & \dfrac{X^2}{100^2}+\dfrac{Y^2}{25^2}=1 \quad \cdots\cdots \text{Case4}
\end{array}\right\} \quad \cdots\cdots\cdots\cdots (1)$$

The following equation[2] was used as the law differentiating crack propagation and J-integral range.

$$da/dN=1.35\times10^{-3}\Delta J^{1.44} \quad \cdots\cdots\cdots\cdots (2)$$

The analysis program for calculating J-integral is MARC-K2.

3. EXPERIMENT AND ANALYSIS

Experimental results on the relationship between crack depth a and aspect ratio a/c are shown in Fig. 4. Aspect ratio a/c increases with crack depth a in the early stage of crack propagation and becomes the maximum value, about 0.37, and then gradually decreases. The relationships between crack depth propagation rate da/dN and crack depth a and between crack length propagation rate dc/dN and half of crack length c are shown in Fig.s 5 and 6 respectively. With crack growth, da/dN decreases and dc/dN increases. This behavior may be characteristic of surface crack growth on a plate subjected to cyclic bending stress. In comparison with base metal and welded joints, the crack growth rate of welded joints is a little higher than that of base metal at the base of the strain range. Many cracks, generally called back surface cracks, initiate by fatigue on the opposite surface from the artificial slit and grow keeping semi-circular shapes in early stages and then gradually grow into slender semi-elliptical shape cracks, sometimes combining with each other, and finally uniting with the main crack growing on the slit side. For comparison, crack propagation rates of semi-circular cracks on a solid bar specimen and side edge cracks on a rectangular plate specimen subjected to push-pull loads are shown in Fig. 5 [3]. The early behavior of back surface crack growth seems similar to the crack growth under push-pull loading.

In comparing base metal to welded joints, as shown in Fig. 7, there is no appreciable difference in the crack propagation behavior of the two materials in either fatigue or creep-fatigue tests. Thus, it is not necessary to distinguish base metal in welded joints in calculating crack growth.

3.2 Measurement of crack shape by Pulse-PDM

Examples of fatigue crack configurations measured non-destructively with the pulse-electric potential drop method using a 10 msec pulse of very large current (1000~1500 A), is shown in Fig. 8(b). In the figure, shapes of beach -marks obtained from fracture surfaces after fatigue tests are shown in order to compare results of P-PDM. The results of non-destructive measurement and fracture surfaces agree. Therefore, it is clear that P-PDM is available for non -destructive detection of part-through surface cracks.

3.3 2-dimensional J-distribution at the fronts of semi-elliptical surface cracks

Analyses of J-integrals were carried out on the 4 cases corresponding to the 4 crack configurations described by eq. (1) and Fig. 3(b). Analytical results on cases 2 and 4 are shown in Fig. 9. To study whether J-integral calculation is rational or not, J-integral analysis is carried out along 8 different paths. It is confirmed that the maximum variation among paths is about 3%. Therefore, there is no appreciable of the calculation path effect on J-integral value.

J-integral increases with applied load and the tendency to increase depends on crack configuration. In a case of a small crack to relative plate thickness, for example, cases 1 and 2, J-integral becomes the minimum value at the plate surface ($\theta=0^\circ$), increases with θ, and is maximum at the deepest point ($\theta=90^\circ$).

In the case of a relatively large crack, such as in case 3, the value of J -integral is constant above $\theta=50^\circ$, and the maximum value exists at $\theta=30^\circ$ ~ 60° in case 4, where crack depth equals half the thickness of the plate.

According to beachmarks on the fracture surface, the crack propagation rate in the thickness direction($\theta=90^\circ$) is larger than that in the width direction ($\theta=0^\circ$). Therefore, it is considered that the analytical behavior of crack growth is similar to the experimental results.

3.4 Analysis of crack growth

Simulation analysis of crack growth is carried out with J-integral obtained from the above analysis. Fig. 10 shows the relationship between crack depth a and length c, and the number of cycles N, as the result of simulation analysis of the crack growth experiment carried out on the base metal under $\Delta\varepsilon=0.4\%$ bending loading.

As the law of crack propagation, eq. (2) is adopted.

$$da/dN=1.35\times10^{-3}\Delta J^{1.44} \quad \cdots\cdots(2)$$

J-integral range, ΔJ, is determined from a J-integral calculated for monotonic loading by two simplified methods. One is $\Delta J=2J$ and the other is $\Delta J=4J$. The results of analysis using these simplified methods are shown in Fig. 10.

Experimental crack depth a agrees with the value obtained by $\Delta J=2J$, and crack length c is simulated well by $\Delta J=4J$ rather than by $\Delta J=2J$.

It seems that the multiplicative factor of J is different depending on the location of the crack front because the crack closure point during a single cycle depends on the crack front location and because it is assumed that cracks

always have the same aspect ratio. It will be future work to clarify the relationship between crack closure behavior and the multiplicative factor of the J-integral.

4. CONCLUSION

In order to study the effectiveness of the non-destructive measurements of surface cracks and analyses of crack growth by inelastic fracture mechanics, the 50 mm thick and 500 mm wide SUS304 stainless steel plates as parent metal and for butt-welded joints were cyclically bent at a temperature of 550℃ under deflection control with simulated of thermal stress. From the results of these tests, the following were obtained.

(1) The pulse electric potential drop method can be used effectively for accurate measuring of surface crack shapes.
(2) When the main crack, starting at the front side of the plate, has progressed through above half the plate thickness, the crack can be regarded as having penetrated through the plate because a counter-crack initiates and comes from the rear side as well.
(3) The results of estimating, with fracture mechanics parameters (J-integral), the propagation behavior of surface cracks due to fatigue coincide precisely with experimental values.

5. ACKNOWLEDGMENTS

This study was performed as one of the activities in the research program "The verification of evaluation method for structural integrity at high-temperature under the sponsorship of Japanese Ministry of International Trade and Industry. The authors would like to express their gratitude to the valuable comments by the members of research committee (Chairman: Prof.Dr.G.Yagawa, Univ. of Tokyo).

REFERENCES

[1] Ishizuki, T., et. al., (1985), Local electrical potential drop method for monitoring micro-crack initiation and growth from weld toes, Journal of the Japanese Society for Non-destructive Inspection, Vol. 34, PP. 583-590.
[2] Saito, M., et. al., (1988), Elevated temperature fracture mechanics approach for an assessment of structural materials for LMFBR, Spring meeting proceedings of the Atomic Energy Society of Japan, P.
[3] Usami, S., et. al., (1986), Micro-crack Initiation, Propagation and Threshold in Elevated Temperature Inelastic Fatigue, Journal of Pressure Vessel Technology, Vol. 108, PP. 214-225.

Table 1 Chemical compositions (%)

C	Si	Mn	P	S	Ni	Cr	Co
0.04	0.56	0.82	0.030	0.005	8.87	18.40	0.04

Table 2 Mechanical properties

	Y.S. σ_Y, 0.2% (MPa)	T.S. σ_u (MPa)	Elong. δ (%)
R.T.	240.0	650.0	62.0
500°C	130.0	380.0	38.0

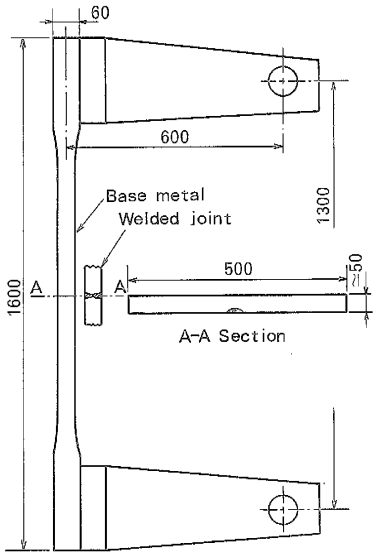

Fig. 1. Configuration of wide plate specimen

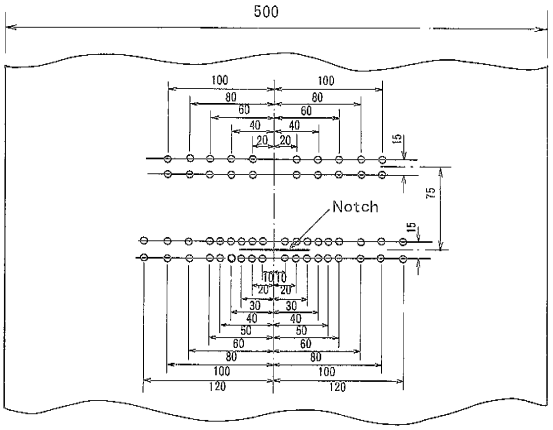

Fig. 2. Position of crack depth measurement by electrical potential drop method

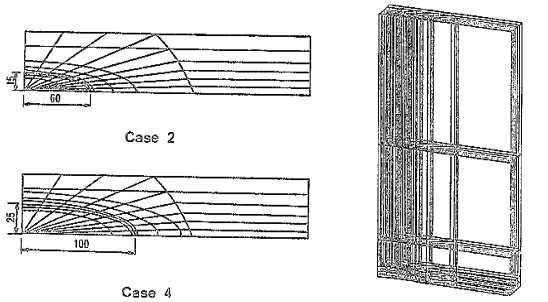

(a) Crack model (b) Finite element mesh

Fig. 3. FEM analysis model

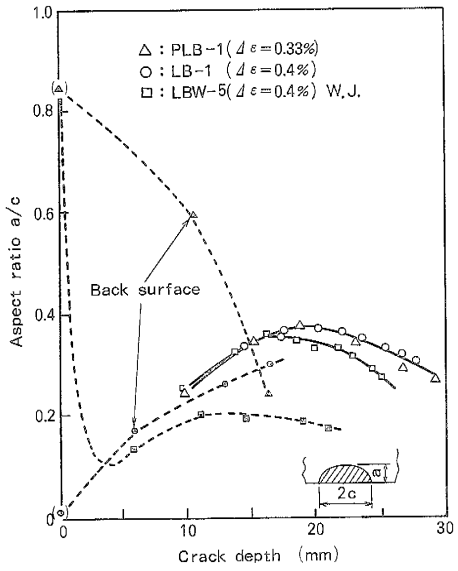

Fig. 4. Relationships between a and a/c (Fatigue)

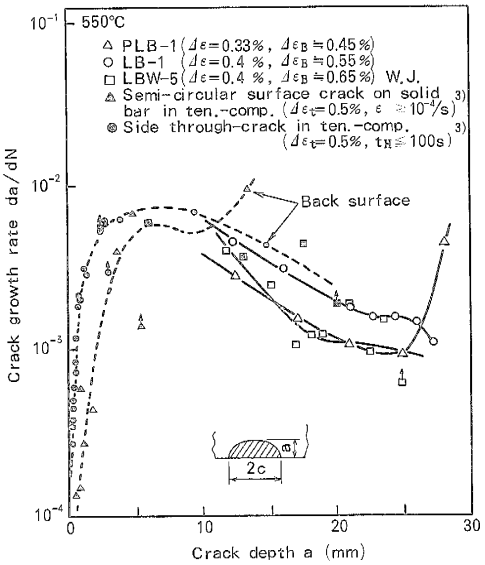

Fig. 5. Relationships between a and da/dN (Fatigue)

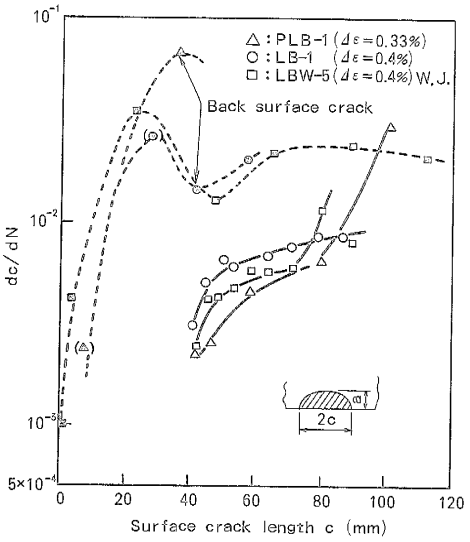

Fig. 6. Relationships between c and dc/dN (Fatigue)

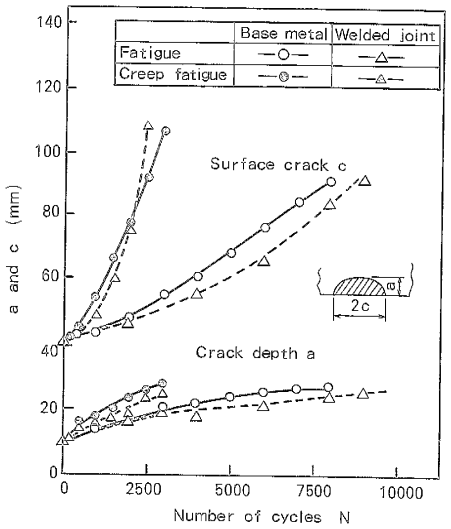

Fig. 7. Comparison of crack growth behavior between base metal and welded joints.

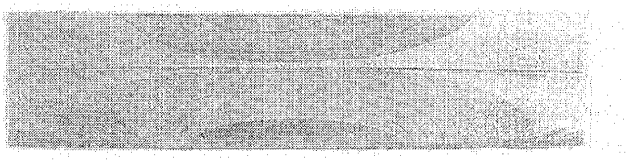

(a) Beach marks on the fracture surface

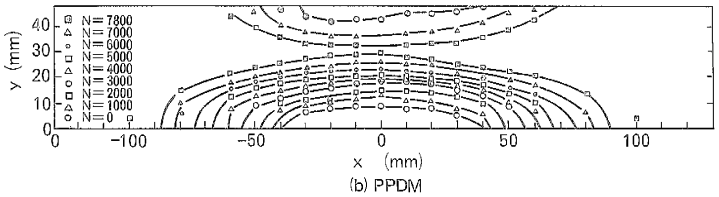

(b) PPDM

Fig. 8. Comparison of crack configurations obtained by PPDM and beach marks

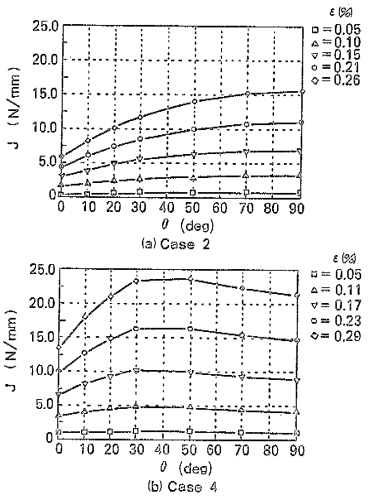

Fig. 9. J-integral distribution along the crack front

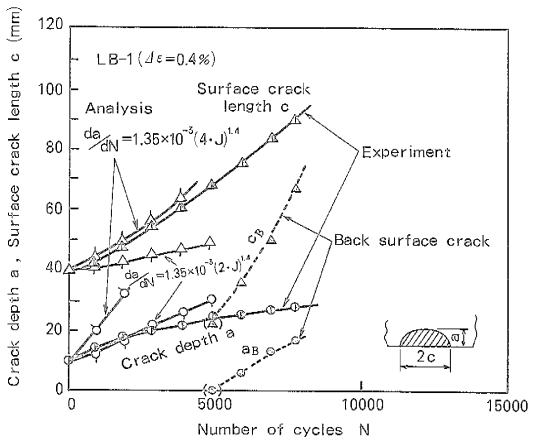

Fig. 10. Comparison of analytical and experimental results on crack propagation